

# Preparation and Electrical Properties of Metal Sulfides–Amidoximated PAN Composite Film

SUNG SOON IM,<sup>\*1</sup> JOON SUNG LEE,<sup>1</sup> and EUN YOUNG KANG<sup>2</sup>

<sup>1</sup>Department of Textile Engineering, College of Engineering, Hanyang University, Seoul, Korea, and <sup>2</sup>Polymer Processing Laboratory, Korea Institute of Science and Technology, Seoul, Korea

## SYNOPSIS

To improve the electrical conductivity of polyacrylonitrile (PAN) film, metallic sulfides and PAN composite film were prepared by the chelating method. Dense PAN film and porous PAN film were prepared by dry process and wet process, respectively. These PAN films were treated to  $\text{NH}_2\text{OH}$  solution to introduce the amidoxime group coordinated with metallic ion.  $\text{Cu}^{+2}$  and  $\text{Cd}^{+2}$  ions were adsorbed to amidoximated PAN films, the sulfur ion was treated with metal-adsorbed PAN films, and thus CuS– and CdS–PAN composite films were prepared. The adsorptive capacity of amidoximated PAN film for the  $\text{Cu}^{+2}$  ion was independent of the morphology of the PAN film, but the adsorptive capacity of the  $\text{Cd}^{+2}$  ion on amidoximated PAN film was dependent on porosity of the polymer. Adsorptive capacity of amidoximated porous PAN film for  $\text{Cd}^{+2}$  was improved about four times than that of amidoximated dense PAN film. The electrical conductivities of CuS–dense and porous PAN composite film were both  $10^{-1}$  S/cm in optimum condition, but because of the difference in adsorptive capacity, the electrical conductivities of CdS–dense and CdS–porous PAN composite films were  $10^{-9}$  S/cm and  $10^{-4}$  S/cm, respectively. Additionally, because CdS was known as a photoconductive material, the photoconductive properties of CdS–porous PAN composite film were investigated.

## INTRODUCTION

In recent years, semiconducting metal sulfides, such as CuS and CdS, have received considerable attention due to their high potential as photoconductors, phosphors, electrodes, etc.<sup>1–5</sup> On the other hand, polymer bearing amidoxime groups, such as ligands, show high adsorptivity to Cu, Cd, and Cr, as well as to uranium in seawater, principally due to the proton-binding and metal-complexing abilities of the ligand.<sup>6–8</sup>

In order to introduce the amidoxime group to PAN film, a cyano group of PAN film was substituted for the amidoxime group by reacting with hydroxylamine under various reaction conditions.

$\text{Cu}^{+2}$  and  $\text{Cd}^{+2}$  ions were adsorbed to amidoximated PAN film and the sulfur ion was treated with

metal-adsorbed PAN film. Thus CuS– and CdS–PAN composite films were prepared.

An adsorption rate of  $\text{Cu}^{+2}$  and  $\text{Cd}^{+2}$  ion on a polymer bearing amidoxime group depends considerably on the morphology of the polymer.<sup>9</sup> Thus, the adsorption rate onto the porous polymer is much higher than that on the gel-type one. In this article, adsorption properties of  $\text{Cu}^{+2}$  and  $\text{Cd}^{+2}$  ions on polymers bearing the amidoxime group were examined especially in regard to the dependence upon porosity of the polymer. The electrical properties of metal sulfide–PAN composite film, especially the photoconductive properties of CdS–porous PAN composite film, were investigated.

## EXPERIMENTAL

### Materials and Reagents

Polyacrylonitrile (Hanil Synthetic Fibers Co., Ltd) was used as a copolymer of 91.5% acrylonitrile, 8%

\* To whom correspondence should be addressed.

methacrylate, and 0.5% sodium methallylsulfonate. All reagents were used without further purification.

### Preparation of PAN Film

In this article, two kinds of PAN film were obtained. Dense PAN film and porous film were prepared by a dry process and a wet process, respectively (Fig. 1). In both cases, PAN cake (20 g) was dissolved in 100 mL of DMF.

### Preparation of Metal Sulfide-PAN Composite Film

Figure 2 shows the schematic diagram of the process of the metal sulfide-PAN composite. PAN film was prepared by the previously mentioned method. Then, to introduce the amidoxime group to PAN film, PAN film was treated with hydroxylamine solution. After the metal ion was introduced to amidoximated PAN film, the sulfur ion was introduced. Finally, metal sulfide-PAN composite film was prepared.

### Amidoximation of PAN Film

PAN film was treated with 5% hydroxylamine (prepared by neutralization of hydroxylamine hydrochloride with NaOH) in deionized water at 40°C for 4 h to afford a polymer bearing amidoxime group. After washing well with water and then being dried *in vacuo*, the polymer was stored in a desiccator.

### Introduction of Metal Ions

Cupric sulfate and cadmium chloride were dissolved in a buffer solution (pH 2, 4, 10) to make a 0.5 M

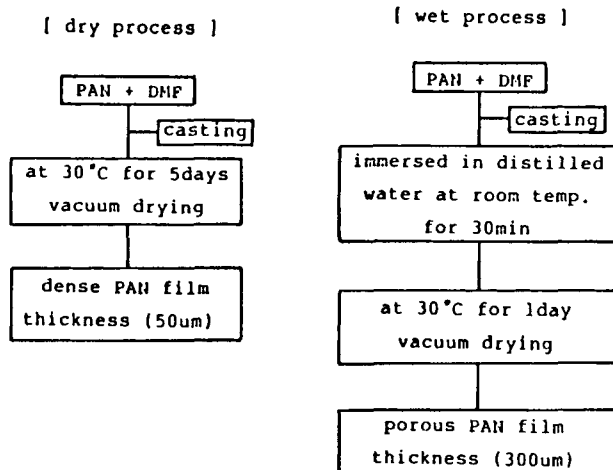


**Figure 1** Schematic diagram of the process of two groups of PAN film preparation.

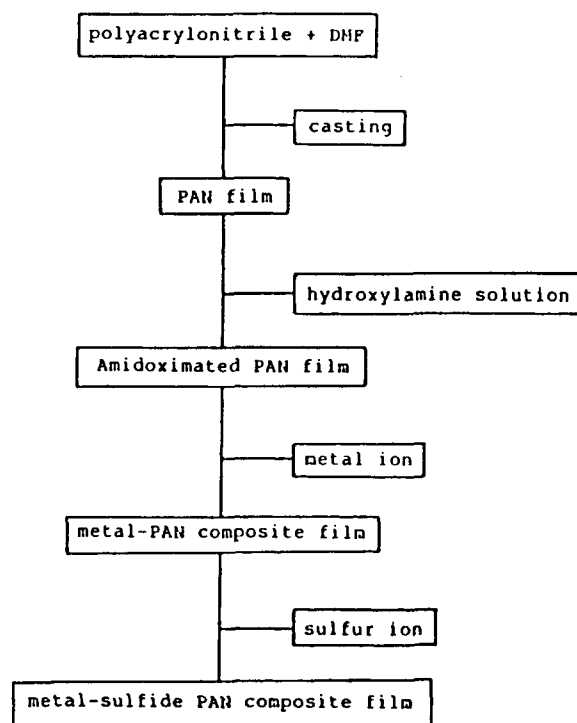


**Figure 2** Schematic diagram of the process of metal-sulfide PAN composite film preparation.

solution. This solution was added to the amidoximated PAN film in a 50 cm<sup>3</sup> vessel (liquor ratio = 1 : 400). The vessel was sealed and maintained at a given temperature for a given period of time, with shaking.

### Introduction of the Sulfur Ion

Excess dry H<sub>2</sub>S gas (prepared by reaction of Na<sub>2</sub>S with H<sub>3</sub>PO<sub>4</sub>) was added to metal introduced PAN film for 1 day at room temperature.

### Adsorptive Capacity for Cu<sup>+2</sup> and Cd<sup>+2</sup>

After the adsorption of the metal ion was complete, the residue solution was diluted with deionized water to make a 10 ppm solution. The adsorptive capacity of the metal ion was determined with a Perkin-Elmer Model 80 atomic absorption spectrophotometer. The adsorptive capacity was evaluated from the difference between the initial and the final concentration of the solution.

### Measurements

The morphology of the metal sulfide-PAN film was investigated with a Jeol JSM-350CF Scanning

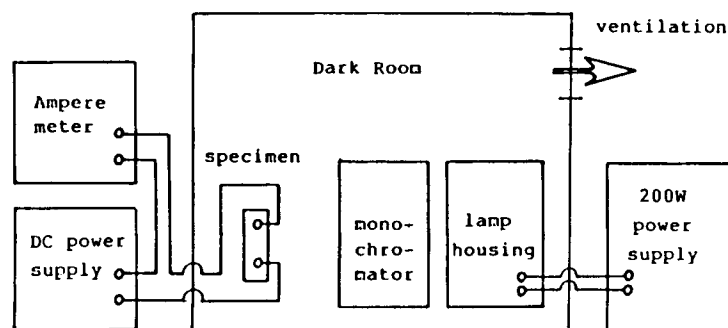


Figure 3 Schematic diagram of the measurement apparatus for photoconductivity.

Electron Microscope. To identify the introduction of the amidoxime group and metal ions, an FT-IR spectrum was obtained using a Nicolet DX FT-IR spectrometer.

#### Temperature Dependence of Conductivity

Temperature dependence of surface and volume conductivity were measured by the four probe and two probe methods, respectively.<sup>10,11</sup>

#### Measurements of Photoconductivity

Photoconductivity for the CdS-PAN composite film was investigated as Figure 3. Wavelength of light irradiated from the lamp housing (Oriol 6605) was controlled by Monochromator (Oriol 77269 monochromator). Spectral distribution of photocurrent was measured by Amperemeter (Keithley 617 Electrometer).

## RESULTS AND DISCUSSION

### The Adsorptive Capacity for $\text{Cu}^{+2}$ and $\text{Cd}^{+2}$

Table I shows the adsorptive capacity of amidoximated PAN film for  $\text{Cu}^{+2}$  and  $\text{Cd}^{+2}$  ions at various conditions. In the case of the  $\text{Cu}^{+2}$  ion, both dense and porous films have maximal adsorptivity at pH 4. But adsorptive properties of the  $\text{Cd}^{+2}$  ion on the amidoximated PAN film are dependent on the porosity of the polymer. The adsorptive capacity of porous PAN film for the  $\text{Cd}^{+2}$  ion was improved about four times that of dense PAN film.

Because the amidoximated PAN film exhibits low adsorptivities for the  $\text{Cd}^{+2}$  ion, amidoximated PAN film was reacted for a few days.

### Structure

Figure 4 shows the SEM of surface and fracture of original dense and porous films. Figure 4(A) exhibits

Table I The Adsorptive Capacity of  $\text{Cu}^{+2}$  and  $\text{Cd}^{+2}$  in Amidoximated PAN Film (mmol/1g-PAN)

Metal	PAN	Reac. Time	pH 2 Reac. Temp.			pH 4 Reac. Temp.			pH 7 Reac. Temp.			pH 10 Reac. Temp.		
			25°C	60°C	95°C	25°C	60°C	95°C	25°C	60°C	95°C	25°C	60°C	95°C
$\text{Cu}^{+2}$	Dense PAN Film	1	82.68	85.76	88.35	88.35	92.30	99.22	88.45	91.91	99.99	84.99	86.16	86.54
		2	84.22	88.07	91.53	89.99	95.76	121.14	88.85	99.22	107.68	86.53	88.27	91.91
		3	86.15	92.30	93.45	91.15	123.07	126.53	94.22	107.68	115.38	88.84	91.93	93.07
	Porous PAN Film	1	84.61	85.76	88.45	90.38	96.15	97.30	89.61	92.30	93.07	86.53	88.07	88.45
		2	85.38	89.61	92.30	100.76	111.53	117.30	92.30	96.53	107.30	88.45	91.15	94.61
		3	88.45	94.61	99.99	110.76	126.91	134.61	96.53	123.07	127.30	92.30	98.07	109.61
$\text{Cd}^{+2}$	Dense PAN Film	1	4.46	8.48	8.92	12.94	15.62	20.08	9.82	12.94	14.73			
		3	6.69	9.82	10.26	14.73	20.08	26.78	13.39	15.17	17.85			
		6	10.26	12.94	13.39	17.85	26.78	29.46	15.62	17.85	21.42			
	Porous PAN Film	1	93.29	95.97	97.31	98.20	106.28	109.81	95.08	102.22	102.67			
		3	103.11	107.13	109.36	111.60	120.52	124.99	107.13	112.93	116.06			
		6	111.60	113.83	116.06	115.17	127.22	133.92	113.83	117.84	119.63			

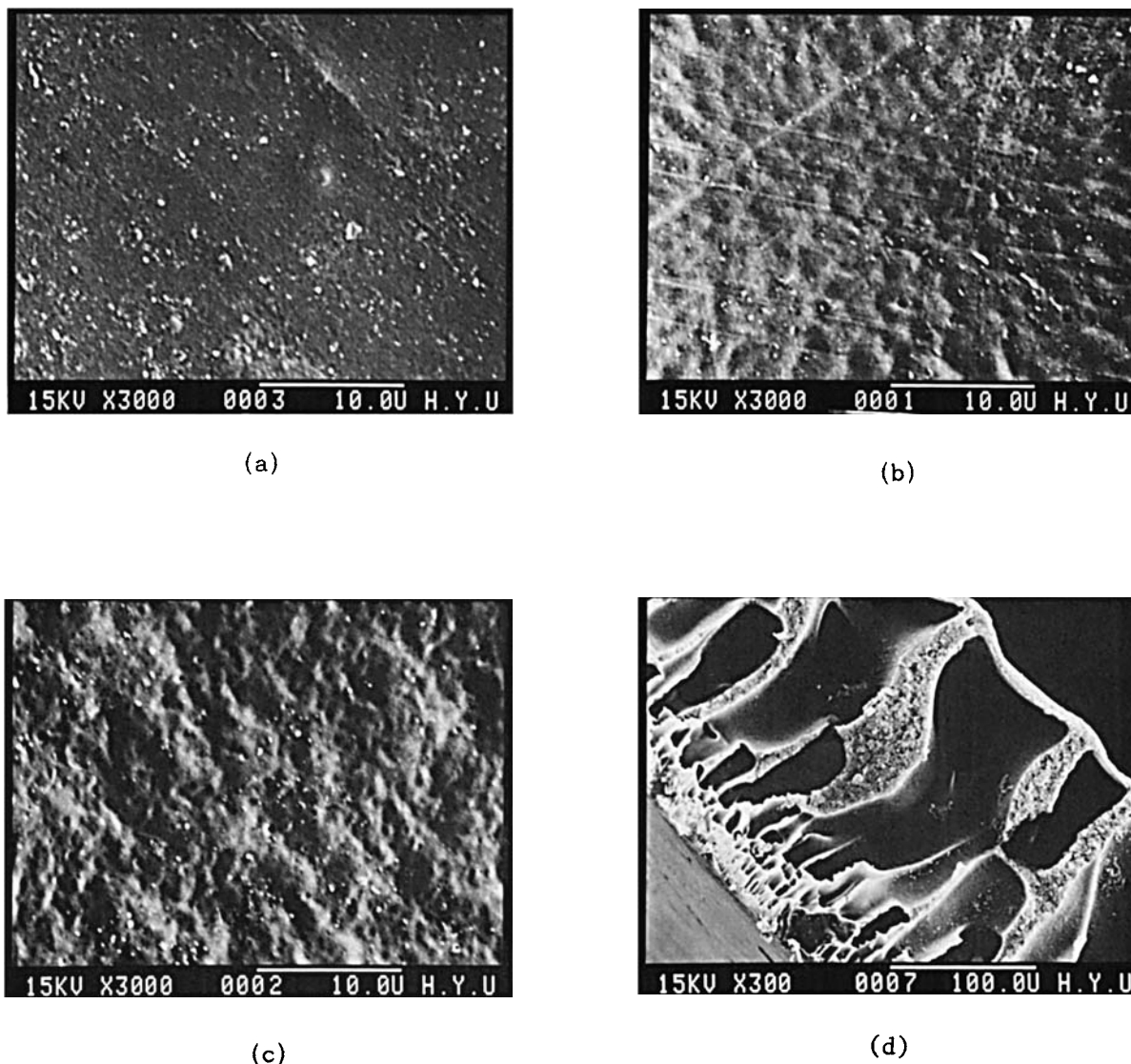


**Figure 4** SEM of (A) the original dense PAN film and (B) the original porous PAN film surface. (C) Liquid side, (D) glass side and fracture.

the surface of dense PAN film and 4(B) and (C) exhibit the liquid side and glass side of porous PAN film, respectively. Figure 4(D) is the fracture of porous PAN film. In Figures 4(B) and (C), we can see that the formed pore is uniformly distributed, but in the case of Figure 4(D), it was found that a finger-like cavity was formed by water-intrusion, due to immersion into nonsolvent water.<sup>12</sup>

#### Variation of Conductivity According to Metal Adsorptivity

In the case of the CuS-PAN composite film, both dense and porous film have maximal conductivity

in pH 4 due to the maximal adsorptivity for the  $\text{Cu}^{+2}$  ion (Fig. 5). The CuS-PAN composite film exhibits maximal conductivity when amidoximated PAN film was treated with copper sulfate at 60°C for 3 h (Fig. 6).

The electrical conductivity was  $10^{-1}$  S/cm in optimum conditions. In the case of CdS-PAN composite film, the electrical conductivities of CdS-dense and CdS-porous PAN composite films were different due to the difference of adsorptive capacity.

Figure 7 exhibits the pH dependence of conductivity for CdS-PAN composite film. Both dense and porous film have maximal conductivity at pH 4. CdS-PAN composite film shows maximal conduc-

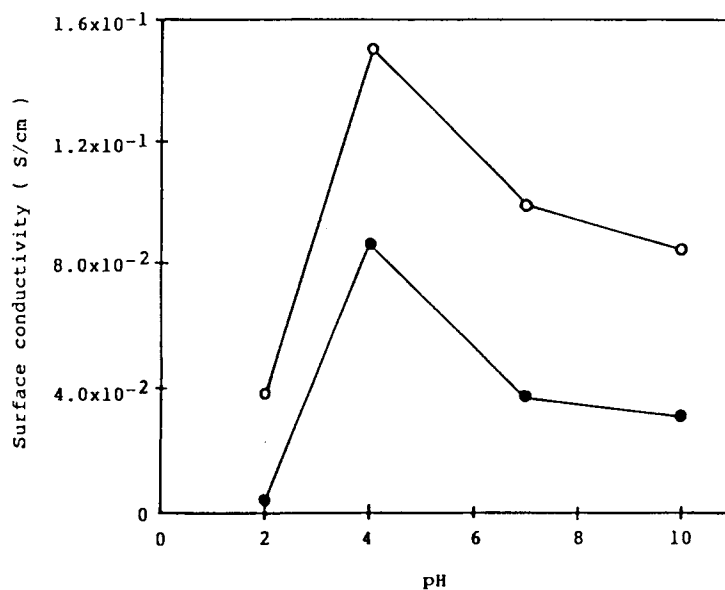
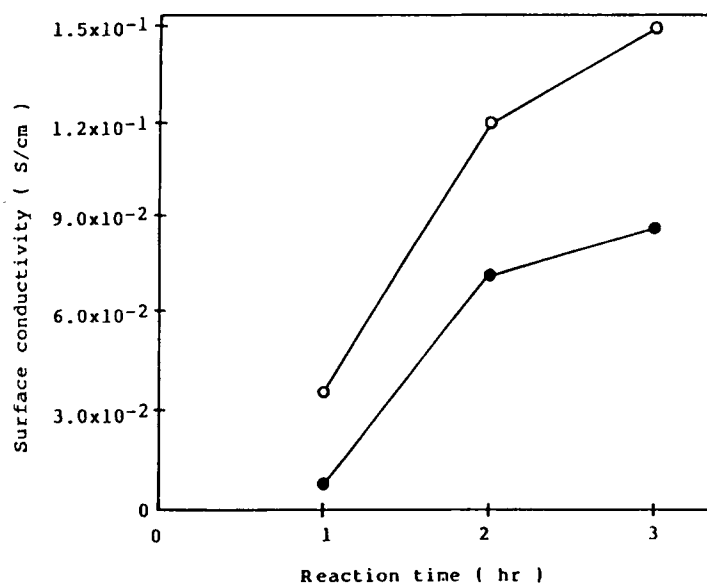


**Figure 5** Surface conductivity of (●) CuS-dense and (○) porous PAN composite film at various pH values.  $\text{CuSO}_4$ : 0.5 M, Reaction time: 3 h, Reaction temp.:  $60^\circ\text{C}$ , Liquor ratio = 1 : 400.

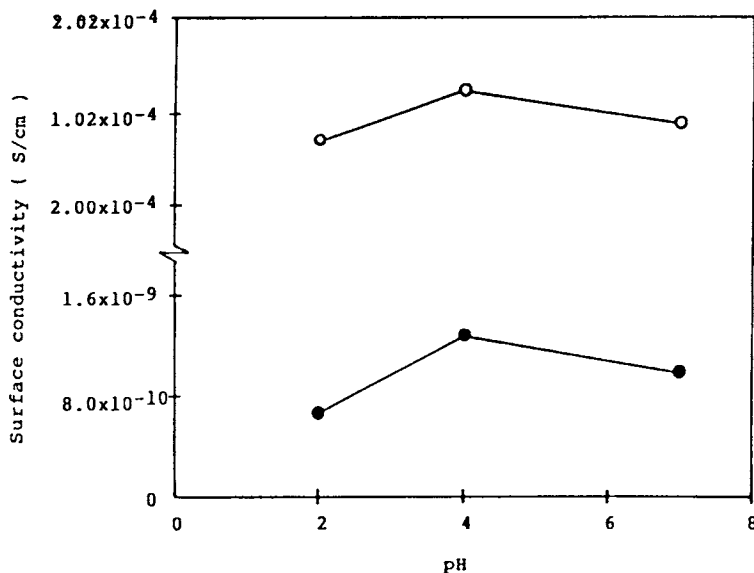
tivity when the amidoximated PAN film was treated with cadmium chloride at  $60^\circ\text{C}$  for 6 days (Figs. 8 and 9). The electrical conductivities of CdS-dense and CdS-porous PAN composite films were  $10^{-9}$  S/cm and  $10^{-4}$  S/cm, respectively, in optimum conditions.

### Characterization

An infrared spectrum of original PAN film was shown in Figure 10 as (—). The characteristic stretching band of nitrile groups appears at  $2240\text{ cm}^{-1}$ . On the other hand, the polymer obtained by



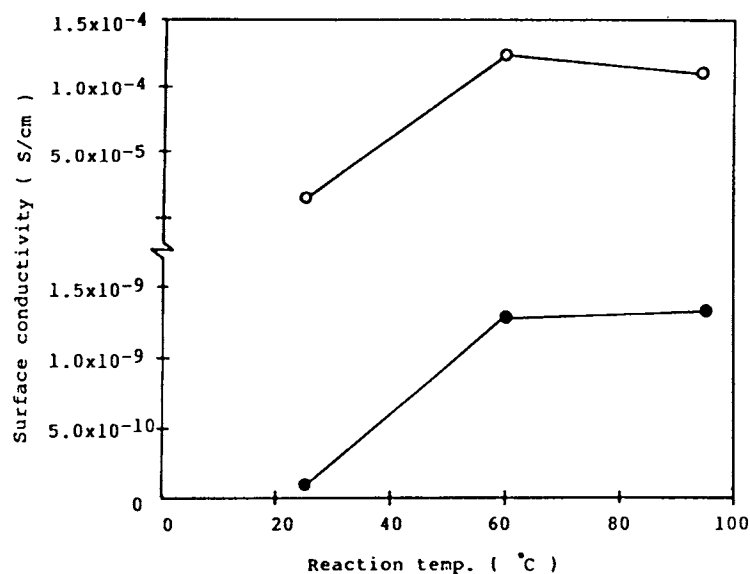
**Figure 6** Surface conductivity of (●) CuS-dense and (○) porous PAN composite film at various reaction times.  $\text{CuSO}_4$ : 0.5 M, pH = 4. Reaction temp.:  $60^\circ\text{C}$ , Liquor ratio = 1 : 400.



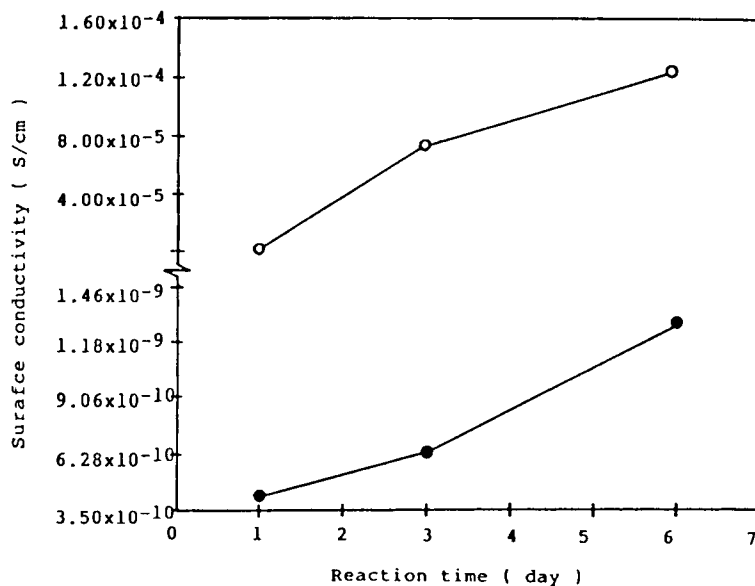
**Figure 7** Surface conductivity of (●) CdS-dense and (○) porous PAN composite film at various pH values.  $\text{CdCl}_2$ : 0.5 M, Reaction time: 6 days, Reaction temp.:  $60^\circ\text{C}$ , Liquor ratio = 1 : 400.

treatment of PAN with hydroxylamine exhibits some new bands accompanied by the reduced adsorption band due to unreacted nitrile groups, as shown in Figure 10 as (---). The bands at  $3460$  and  $3390\text{ cm}^{-1}$  are assigned to an asymmetric and a symmetric stretching mode of  $\text{NH}_2$  groups, respec-

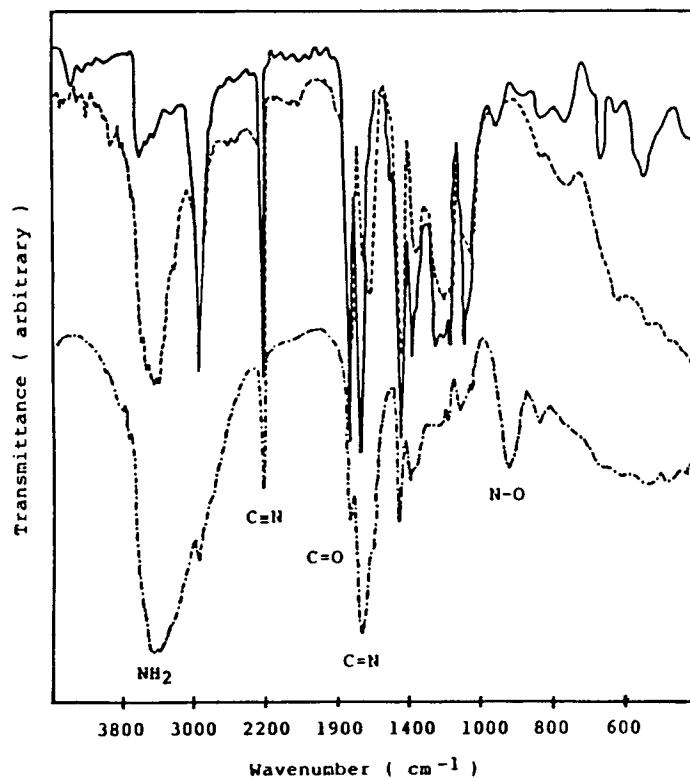
tively. The bands at  $1660$  and  $920\text{ cm}^{-1}$  are assigned to a  $\text{C}=\text{N}$  stretching mode and a  $\text{N}-\text{O}$  stretching mode of oxime groups, respectively.<sup>7,13</sup> These results show clearly the extensive conversion of the original nitrile groups to amidoxime groups through the treatment with hydroxylamine.



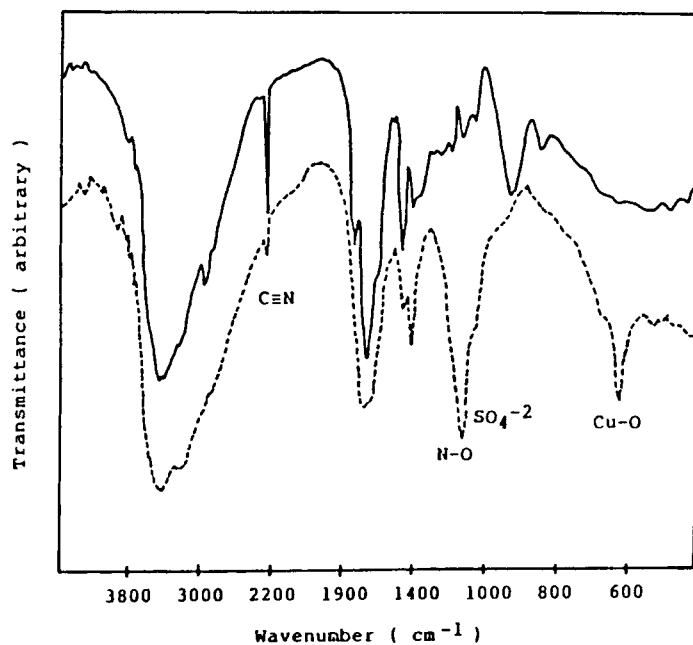
**Figure 8** Surface conductivity of (●) CdS-dense and (○) porous PAN composite film at various reaction temperatures.  $\text{CdCl}_2$ : 0.5 M, Reaction time: 6 days, Liquor ratio = 1 : 400.



**Figure 9** Surface conductivity of (●) CdS-dense and (○) porous PAN composite film at various reaction times.  $\text{CdCl}_2$ : 0.5 M, pH = 4, Reaction temp.: 60°C, Liquor ratio = 1 : 400.



**Figure 10** IR spectra of (—) original dense PAN film, (----) original porous PAN film and (-·-) amidoximated PAN film.



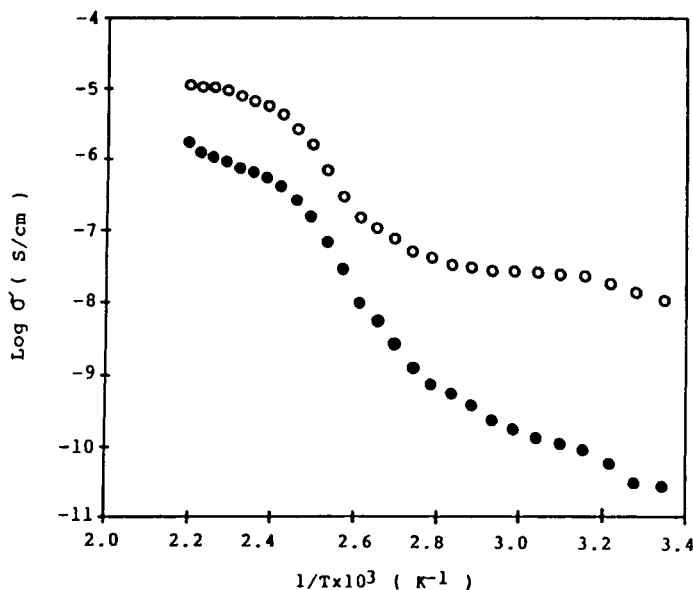
**Figure 11** IR spectra of (—) amidoximated PAN film and (----) CuS-PAN composite film.

Figure 11 shows the FT-IR spectra of amidoximated PAN film (—) and Cu-PAN composite film (----). Compared with the spectrum of amidoximated PAN film, the CN group band ( $2245\text{ cm}^{-1}$ ) is strongly reduced in the spectrum of Cu-PAN composite film. The N—O peak coordinated with metal appears at  $1110\text{--}1200\text{ cm}^{-1}$ . The  $\text{SO}_4^{2-}$

peak and Cu—O peaks also appear at  $1000\text{--}1100\text{ cm}^{-1}$  and  $620\text{ cm}^{-1}$ , respectively.<sup>14,15</sup>

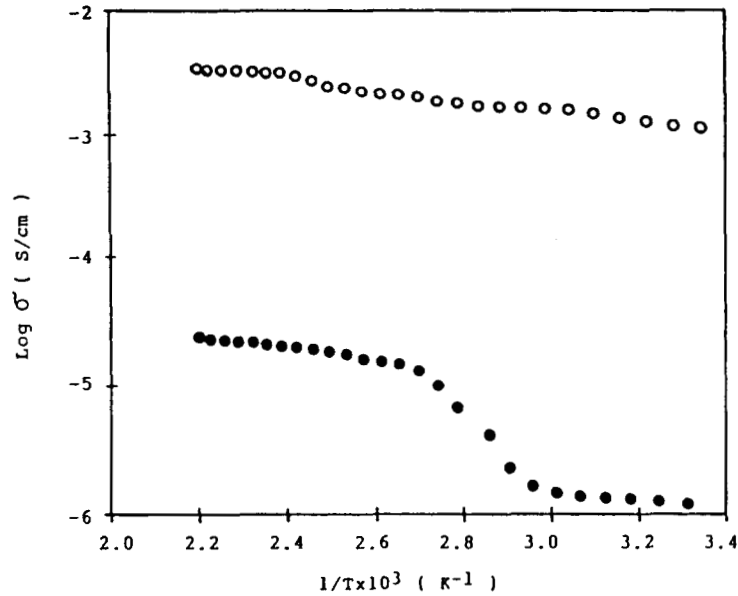
#### Electrical Properties of CuS-PAN Composite Film

Figure 12 shows the temperature dependence of surface conductivity of CuS-dense and porous PAN



**Figure 12** Temperature dependence of surface conductivity for (●) CuS-dense and (○) porous PAN composite film.





**Figure 13** Temperature dependence of bulk conductivity for (●) CuS-dense and (○) porous PAN composite film.

composite film. The conductivity curve is similar to that of the CuS crystal.<sup>16-18</sup> Therefore, the surface conductivity of the CuS-PAN composite film is considered to be due to a CuS network on the surface of the film.

Figure 13 shows the temperature dependence of bulk conductivity of CuS-dense and porous PAN

composite film. In the case of CuS-dense PAN film, the charge carrier trapped in matrix was detrapped by thermal activation of PAN and contributed to conduction. Therefore, the conductivity of sample was abruptly changed in the vicinity of  $T_g$ .<sup>19</sup> But in the case of the CuS-porous PAN film, conductivity was not dependent on matrix PAN.

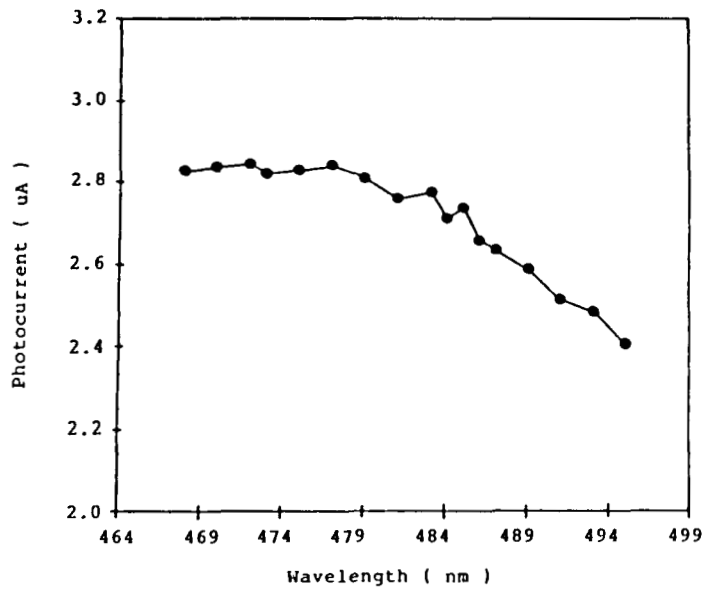


**Figure 14** Curves of spectral photocurrent distribution of CdS-porous PAN composite film produced by illumination at the induced wavelength.

Electrical properties of CdS-PAN composite film were very similar to those of CuS-PAN composite film.

### Photoconductive Properties of CdS-, Porous PAN Composite Film

A great number of compounds are now known to have the fine structure of photocurrent that results from the exciton contribution into conductivity. CdS crystals can be divided into two groups.<sup>20-22</sup> In the crystals of the first group, 77°K maxima of the photocurrent corresponds to absorption lines, whereas in the crystals of the second group, the minima corresponds to the same absorption lines. The difference between the two groups of crystals can be understood in terms of photoactive and, consequently, photoinactive decay of excitons.

Serving as recombination centers for free carriers (dissociated excitons included), the oxygen adsorbed accounts for the decrease in the carrier density at the surface and the appearance of minima in the photoconductivity curve (second group crystals). Desorption of oxygen produces a decrease of surface recombination rate and, consequently, an increase in the exciton contribution into the conductivity. Photoactive decay of excitons at the surface results in the appearance of maxima in the photocurrent distribution curve (first group crystals).

Figure 14 shows the distribution of photocurrent of CdS-porous PAN composite film according to wavelength. From results of minima at 473, 480, and 484 nm, it is known that the oxygen is involved. Further investigation on photoconductivity will be discussed in future articles.

This work was carried out under a research grant from the Korea Science and Engineering Foundation (860515, 890415).

### REFERENCES

1. A. M. Andrews and C. R. Haden, *Proc. IEEE*, **57**, 99 (1969).
2. M. Aven and D. M. Cook, *J. Appl. Phys.*, **32**, 960 (1961).
3. F. A. Shirland, *Adv. Energy Conv.*, **6**, 201 (1966).
4. W. H. Bloss and G. Hewig, *14th IEEE Photovoltaic Spec. Conf.*, San Diego (1980).
5. S. Matsumoto, *J. Appl. Phys. Japan*, **11**, 2051 (1979).
6. T. Hirotsu, *J. Chem. Soc. Dalton Trans.*, 1609 (1986).
7. T. Hirotsu, *Ind. Eng. Chem. Res.*, **26**, 1970 (1987).
8. T. Hirotsu, *Sep. Sci. Technol.*, **21**, 1101 (1986).
9. T. Hirotsu, *J. Polym. Sci. Polym. Chem. Ed.*, **24**, 1953 (1986).
10. A. R. Blythe, *Polym. Test.*, **4**, 195 (1984).
11. A. R. Blythe, *Electrical Properties of Polymers*, Cambridge University Press, Cambridge, UK, 1979.
12. R. E. Kesting, *Synthetic Polymeric Membrane*, Wiley, New York, 1985.
13. T. Hirotsu, *J. Appl. Polym. Sci.*, **36**, 1741 (1988).
14. C. N. Rao, *Chemical Applications of Infrared Spectroscopy*, Academic, New York, 1963.
15. E. Kalalova and Z. Radova, *Euro. Polym. J.*, **13**, 293 (1977).
16. K. Okamoto and S. Kawai, *Japan J. Appl. Phys.*, **12**, 1130 (1973).
17. R. T. Shuey, *Semiconducting Ore-Minerals*, Elsevier, Amsterdam, 1975.
18. J. B. Wagner and C. Wagner, *J. Chem. Phys.*, **26**, 1602 (1957).
19. D. A. Seanor, *Electrical Properties of Polymers*, Academic, New York, 1982.
20. E. F. Gross and B. V. Novikov, *J. Phys. Chem. Solids*, **22**, 87 (1961).
21. S. Nikitine, *J. Phys. Chem.*, **69**, 745 (1965).
22. P. Mark and I. D. Levine, *Phys. Rev.*, **144**, 751 (1966).

Received February 27, 1991

Accepted August 28, 1991